ISSN 1674-1056
http://cpb.iphy.ac.cn
http://iopscience.iop.org/cpb
中国物理 B
Chinese Physics
中国物理
Chinese Physics B

Reflected and transmitted powers of arbitrarily polarized plane waves at interface between chiral and achiral media

Lu Yan-Feng(路彦峰), Han Yi-Ping(韩一平)

Citation: Chin. Phys. B . 2019, 28(2): 024202. **doi:** 10.1088/1674-1056/28/2/024202
Journal homepage: http://cpb.iphy.ac.cn; http://iopscience.iop.org/cpb

What follows is a list of articles you may be interested in

Propagation characteristics of oblique incidence terahertz wave through non-uniform plasma

Antao Chen(陈安涛), Haoyu Sun(孙浩宇), Yiping Han(韩一平), Jiajie Wang(汪加洁), Zhiwei Cui(崔志伟)
Chin. Phys. B . 2019, 28(1): 014201. **doi:** 10.1088/1674-1056/28/1/014201

Generation of Mathieu beams using angular pupil modulation

Zhijun Ren(任志君), Jinping He(何晋平), Yile Shi(施逸乐)
Chin. Phys. B . 2018, 27(12): 124201. **doi:** 10.1088/1674-1056/27/12/124201

Further analysis of scintillation index for a laser beam propagating through moderate-to-strong non-Kolmogorov turbulence based on generalized effective atmospheric spectral model

Jing Ma(马晶), Yu-Long Fu(付玉龙), Si-Yuan Yu(于思源), Xiao-Long Xie(谢小龙), Li-Ying Tan(谭立英)
Chin. Phys. B . 2018, 27(3): 034201. **doi:** 10.1088/1674-1056/27/3/034201

(3+1)-dimensional localized self-accelerating Airy elegant Ince-Gaussian wave packets and their radiation forces in free space

Dongdong Li(李冬冬), Xi Peng(彭喜), Yulian Peng(彭玉莲), Liping Zhang(张丽萍), Xingyu Chen(陈星宇), Jingli Zhuang(庄经立), Fang Zhao(赵方), Xiangbo Yang(杨湘波), Dongmei Deng(邓冬梅)
Chin. Phys. B . 2017, 26(12): 124202. **doi:** 10.1088/1674-1056/26/12/124202

Characteristics of photonic nanojets from two-layer dielectric hemisphere

Yunyue Liu(刘昀玥), Xianchao Liu(刘贤超), Ling Li(李玲), Weidong Chen(陈卫东), Yan Chen(陈艳), Yuerong Huang(黄跃容), Zhengwei Xie(谢征微)
Chin. Phys. B . 2017, 26(11): 114201. **doi:** 10.1088/1674-1056/26/11/114201

Reflected and transmitted powers of arbitrarily polarized plane waves at interface between chiral and achiral media*

Yan-Feng Lu(路彦峰)[1,2,†] and Yi-Ping Han(韩一平)[1,‡]

[1] School of Physics and Optoelectronic Engineering, Xidian University, Xi'an 710071, China
[2] School of Physics and Electronic Information, Huaibei Normal University, Huaibei 235000, China

(Received 9 September 2018; revised manuscript received 21 November 2018; published online 10 January 2019)

A study has been made on the reflected and transmitted powers generated when an arbitrarily polarized plane wave impinges at a planar interface separating an isotropic achiral medium (IAM) and an isotropic chiral medium (ICM). It follows that the theoretical formulas are derived for the normalized reflection and transmission powers from an IAM–ICM interface for an arbitrary polarized incident wave, and those at an ICM–IAM interface for right-hand circularly polarized (RCP) or left-hand circularly polarized (LCP) incident wave are also obtained. The behavior of the reflected and transmitted waves in different cases is studied, and the dependence of the reflection/transmission of the incident wave on the incident angle and the parameters of the media is investigated in detail. Our numerical results show that high transmission is exhibited under the impedance matching condition and the incident wave can be split into two waves of the same circular polarization state in the case of the ICM–IAM interface, which indicates that circular polarizing beam splitter is achieved.

Keywords: chiral media, reflection power, transmission power, Fresnel coefficient

PACS: 42.25.Bs, 78.20.ci, 42.25.Gy **DOI:** 10.1088/1674-1056/28/2/024202

1. Introduction

Chiral materials are advantageous in many respects compared with the general materials due to the extra degree of freedom offered by the presence of chiral parameter. Since the time of the optical activity in quartz crystals was first discovered by Arago in the early nineteenth century, chiral materials continue to be of great interest to many researchers owing to their associated electromagnetic properties and potential applications in various areas of basic research and applied research.[1–6] Important attention has been focused on the interaction of electromagnetic waves with chiral structures. Scattering by arbitrarily shaped chiral objects was investigated,[7–10] and novel chiral metamaterials which exhibit new properties have been designed.[11,12]

The optical properties of chiral media are one of the main aspects in the research of chiral materials over the years. The reflection and transmission characteristics at a planar IAM–ICM interface were investigated by Bassiri *et al.*[13] Reflection and transmission of an incident plane wave at the ICM–IAM interface were analyzed by Cory and Rosenhouse,[14] the reflection and transmission coefficients against the incidence angle of the left-hand circularly polarized wave were simulated. Extensions to characteristics of reflected and transmitted waves by chiral slabs,[15] at an ICM–ICM interface,[16,17] and of chiral multilayer structures,[18] were also discussed. The reflection and transmission properties of the incident plane wave at the surface of a chiral negative refraction medium,[19] at the planar isotropic chiral–uniaxial anisotropic chiral interface,[20,21] and from a uniaxial chiral slab,[22] were also investigated in recent years.

Although a number of studies on the properties of the electromagnetic waves propagating in an ICM have been conducted,[13–18,23–33] to our knowledge, energy relation expressions at the surface of a chiral medium for a monochromatic plane wave with arbitrary polarization are not available in the literature. In this paper, characteristics of an electromagnetic wave propagating in the ICM are discussed on the basis of the Post–Jaggard constructive equations. The formulas of normal component of the time-averaged Poynting vectors of the incident, the reflected, and the transmitted waves across a planar interface between an IAM and an ICM are derived. It follows that the normalized power formulas of the reflected and transmitted waves at the IAM–ICM interface for a plane wave at any azimuthal angle are obtained, the power expressions at the ICM–IAM interface for a right-hand circularly polarized (RCP) or left-hand circularly polarized (LCP) incident wave are given as well. Finally, numerical results are presented for three different cases, where the effects of the incident angle, the chiral parameter, and the permittivity on the behavior of the reflection and transmission powers are investigated in detail.

*Project supported by the National Natural Science Foundation of China (Grant Nos. 61431010 and 61501350) and the National Key Basic Research Program of China (Grant No. 2014CB340203).

†Corresponding author. E-mail: fenghua8820@126.com
‡Corresponding author. E-mail: yphan@xidian.edu.cn

© 2019 Chinese Physical Society and IOP Publishing Ltd

2. Properties of plane wave at the interface between IAM and ICM

Although different sets of constitutive relations were proposed to describe chiral medium in literature,[34–36] mathematical equivalence among these equations can be obtained. In this paper, the following constitutive relations for time-harmonic fields ($\exp(-\mathrm{i}\omega t)$) are adopted

$$\boldsymbol{D} = \varepsilon_\mathrm{c}\boldsymbol{E} - \mathrm{j}\gamma_\mathrm{c}\boldsymbol{B}, \quad \boldsymbol{H} = \boldsymbol{B}/\mu_\mathrm{c} - \mathrm{j}\gamma_\mathrm{c}\boldsymbol{E}, \tag{1}$$

where the scalar parameters ε_c, μ_c, and γ_c denote the permittivity, the permeability, and the chiral parameter, respectively. One should be noted that the value of γ_c is a measure of the handedness of the chiral medium, which provides direct coupling of the electric and the magnetic fields. In general, there are two distinct waves propagating inside the chiral medium, namely, the RCP wave with wave number $k_\mathrm{R} = \omega\left(\sqrt{\mu_\mathrm{c}^2\gamma_\mathrm{c}^2 + \varepsilon_\mathrm{c}\mu_\mathrm{c}} + \mu_\mathrm{c}\gamma_\mathrm{c}\right)$ and the LCP wave with wave number $k_\mathrm{L} = \omega\left(\sqrt{\mu_\mathrm{c}^2\gamma_\mathrm{c}^2 + \varepsilon_\mathrm{c}\mu_\mathrm{c}} - \mu_\mathrm{c}\gamma_\mathrm{c}\right)$.

2.1. Reflection and transmission at the IAM–ICM interface

As shown in Fig. 1(a), a linearly polarized plane wave is incident from an IAM upon the surface of an ICM at an incident angle θ_i. The continuity of the tangential components of the electric and the magnetic wave vectors at the IAM–ICM interface lead to

$$k_\mathrm{i}\sin\theta_\mathrm{i} = k_\mathrm{r}\sin\theta_\mathrm{r} = k_\mathrm{R}\sin\theta_\mathrm{R} = k_\mathrm{L}\sin\theta_\mathrm{L}, \tag{2}$$

where $k_\mathrm{i} = \omega\sqrt{\mu_\mathrm{a}\varepsilon_\mathrm{a}}$ and $k_\mathrm{r} = k_\mathrm{i}$ are wave numbers of the incident and reflected waves, respectively. θ_R and θ_L are transmitted angles of the RCP and LCP waves, respectively. Critical angles of incidence θ_cL and θ_cR are derived as $\theta_\mathrm{cR} = \sin^{-1}(k_\mathrm{R}/k_\mathrm{i})$ and $\theta_\mathrm{cL} = \sin^{-1}(k_\mathrm{L}/k_\mathrm{i})$, respectively.

It should be noted that the investigation is restricted to $\gamma_\mathrm{c} > 0$ in this paper. As a result, $k_\mathrm{R} > k_\mathrm{L}$ and $\theta_\mathrm{cR} > \theta_\mathrm{cL}$ are valid for all cases. When $\theta_\mathrm{i} > \theta_\mathrm{cL}$, only the RCP wave propagates in the chiral medium, $\cos\theta_\mathrm{R}$ is real and $\cos\theta_\mathrm{L}$ is pure imaginary. Whereas if $\theta_\mathrm{i} > \theta_\mathrm{cR}$, both the two transmitted waves become evanescent, the phenomenon of total internal reflection occurs, both $\cos\theta_\mathrm{R}$ and $\cos\theta_\mathrm{L}$ are pure imaginary numbers.

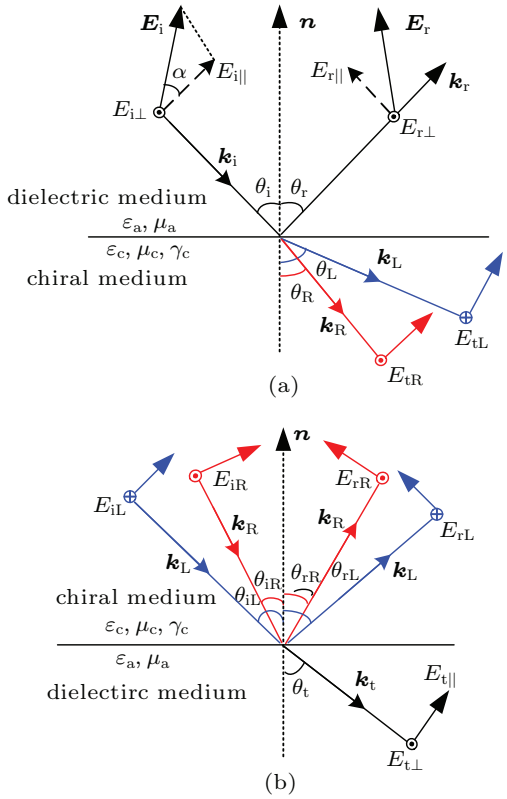


Fig. 1. Reflection and transmission at the interface of two different media: (a) achiral–chiral, (b) chiral–achiral.

Considering the relations $k_\mathrm{c} = \omega\sqrt{\mu_\mathrm{c}\varepsilon_\mathrm{c}}$ and $\gamma_{\mathrm{c}0} = |\varepsilon_\mathrm{c}\mu_\mathrm{c} - \varepsilon_\mathrm{a}\mu_\mathrm{a}|/2\mu_\mathrm{c}\sqrt{\varepsilon_\mathrm{a}\mu_\mathrm{a}}$, when $0 < \gamma_\mathrm{c} < \gamma_{\mathrm{c}0}$ and if $k_\mathrm{i} < k_\mathrm{c}$, there is $k_\mathrm{i} < k_\mathrm{L} < k_\mathrm{R}$, both the RCP and LCP waves propagate in the chiral medium at the range of entire incident angle. Whereas if $k_\mathrm{i} > k_\mathrm{c}$, we have $k_\mathrm{L} < k_\mathrm{R} < k_\mathrm{i}$, the LCP and RCP waves become evanescent for $\theta_\mathrm{i} > \theta_\mathrm{cL}$ and $\theta_\mathrm{i} > \theta_\mathrm{cR}$, respectively. As for $\gamma_\mathrm{c} > \gamma_{\mathrm{c}0}$, we can obtain $k_\mathrm{L} < k_\mathrm{i} < k_\mathrm{R}$, the LCP wave propagates for $\theta_\mathrm{i} < \theta_\mathrm{cL}$ and becomes evanescent for $\theta_\mathrm{i} > \theta_\mathrm{cL}$.

Using the boundary conditions and Snell's law, the amplitudes of the reflected and transmitted waves to the incident components are related by

$$\begin{bmatrix} E_{\mathrm{r}\perp} \\ E_{\mathrm{r}\parallel} \end{bmatrix} = \begin{bmatrix} R_{11} & R_{12} \\ R_{21} & R_{22} \end{bmatrix} \begin{bmatrix} E_\mathrm{i}\cos\alpha \\ E_\mathrm{i}\sin\alpha \end{bmatrix}, \quad \begin{bmatrix} E_\mathrm{tR} \\ E_\mathrm{tL} \end{bmatrix} = \begin{bmatrix} T_{11} & T_{12} \\ T_{21} & T_{22} \end{bmatrix} \begin{bmatrix} E_\mathrm{i}\cos\alpha \\ E_\mathrm{i}\sin\alpha \end{bmatrix}, \tag{3}$$

$$\begin{bmatrix} R_{11} & R_{12} \\ R_{21} & R_{22} \end{bmatrix} = \frac{4g}{\Delta}\begin{bmatrix} (c_\mathrm{i}-c_\mathrm{R})(c_\mathrm{i}+c_\mathrm{L}) & 0 \\ 0 & (c_\mathrm{i}+c_\mathrm{R})(c_\mathrm{i}-c_\mathrm{L}) \end{bmatrix} - \frac{2A}{\Delta}\begin{bmatrix} 0 & 1 \\ 1 & 0 \end{bmatrix}, \tag{4}$$

$$\begin{bmatrix} T_{11} & T_{12} \\ T_{21} & T_{22} \end{bmatrix} = \frac{4c_\mathrm{i}}{\Delta}\left[(1+g)\begin{bmatrix} (c_\mathrm{i}+c_\mathrm{L}) & 0 \\ 0 & (c_\mathrm{i}+c_\mathrm{R}) \end{bmatrix} + (1-g)\begin{bmatrix} 0 & (c_\mathrm{i}-c_\mathrm{L}) \\ (c_\mathrm{i}-c_\mathrm{R}) & 0 \end{bmatrix}\right], \tag{5}$$

where $\alpha = \tan^{-1}\left(E_{\mathrm{i}\perp}/E_{\mathrm{i}\parallel}\right)$ represents the azimuthal angle of the incident wave. The elements R_{ij} and T_{ij} with $i = 1,2$ and $j = 1,2$ indicate the reflection and the transmission coefficients. $\Delta = (1+g)^2(c_\mathrm{i}+c_\mathrm{R})(c_\mathrm{i}+c_\mathrm{L}) - (1-g)^2(c_\mathrm{i}-c_\mathrm{R})(c_\mathrm{i}-c_\mathrm{L})$, $c_\mathrm{i} = \cos\theta_\mathrm{i}$, $c_\mathrm{R} = \cos\theta_\mathrm{R}$, $c_\mathrm{L} = \cos\theta_\mathrm{L}$, $g = \sqrt{(\varepsilon_\mathrm{c}/\mu_\mathrm{c} + \gamma_\mathrm{c}^2)/(\varepsilon_\mathrm{a}/\mu_\mathrm{a})}$, and $A = c_\mathrm{i}(c_\mathrm{R}+c_\mathrm{L})(1-g^2)$.

2.2. Reflection and transmission at the ICM–IAM interface

At the ICM–IAM interface, an RCP (LCP) wave strikes on the interface with an incident angle θ_{iR} (θ_{iL}). As shown in Fig. 1(b), the two reflected waves, namely, the RCP and LCP waves, propagate back into the ICM, and a transmitted wave proceeds in the IAM.

Considering phase matching conditions of the wave vectors at the ICM–IAM interface,[14,23] we find

$$k_R \sin\theta_{iR} = k_R \sin\theta_{rR} = k_L \sin\theta_{rL} = k_t \sin\theta_t, \tag{6}$$

where $k_t = \omega\sqrt{\mu_a\varepsilon_a}$ indicates wave number of the transmitted wave. θ_{rR} and θ_{rL} are reflected angles of the RCP and LCP waves, respectively. θ_t is the transmitted angle. By letting $\theta_t = \pi/2$, critical angles of incidence θ_{cR} and θ_{cL} are given by $\theta_{cR} = \sin^{-1}(k_t/k_R)$ and $\theta_{cL} = \sin^{-1}(k_t/k_L)$, respectively.

As for the case of an RCP incident wave, considering the relation $\theta_c = \sin^{-1}(k_L/k_R)$, when $0 < \gamma_c < \gamma_{c0}$, and if $k_t < k_c$, we have $k_t < k_L < k_R$. If $\theta_{cR} < \theta_{iR} < \theta_c$, no transmitted wave exists, the phenomenon of total internal reflection occurs. Whereas if $\theta_{iR} > \theta_c$, the reflected LCP wave becomes evanescent. But for the case of $k_t > k_c$, we have $k_L < k_R < k_t$, the reflected LCP wave becomes evanescent for $\theta_{iR} > \theta_c$. When $\gamma_c > \gamma_{c0}$, we can obtain $k_L < k_t < k_R$. If $\theta_c < \theta_{iR} < \theta_{cR}$, the reflected LCP wave becomes evanescent. Whereas if $\theta_{iR} > \theta_{cR}$, the total internal reflection occurs.

As for the case of an LCP incident wave, $k_R \sin\theta_{iR}$ in Eq. (6) is replaced with $k_L \sin\theta_{iL}$. The propagation of the reflected and transmitted waves at the interface can be obtained in a similar manner.

Then the relationships of the reflected and transmitted electric fields to the incident components can be expressed by matrices

$$\begin{bmatrix} E_{rR} \\ E_{rL} \end{bmatrix} = \begin{bmatrix} R'_{11} & R'_{12} \\ R'_{21} & R'_{22} \end{bmatrix} \begin{bmatrix} E_{iR} \\ E_{iL} \end{bmatrix}, \quad \begin{bmatrix} E_{t\perp} \\ E_{t\parallel} \end{bmatrix} = \begin{bmatrix} T'_{11} & T'_{12} \\ T'_{21} & T'_{22} \end{bmatrix} \begin{bmatrix} E_{iR} \\ E_{iL} \end{bmatrix}, \tag{7}$$

$$\begin{bmatrix} R_{11} & R_{12} \\ R_{21} & R_{22} \end{bmatrix} = \frac{A}{\Delta} \begin{bmatrix} 1 & 0 \\ 0 & -1 \end{bmatrix} - \frac{B}{\Delta} \begin{bmatrix} 0 & c_{iL} \\ c_{iR} & 0 \end{bmatrix} + \frac{4g}{\Delta} \begin{bmatrix} (c_{iR}-c_t)(c_{iL}+c_t) & 0 \\ 0 & (c_{iR}+c_t)(c_{iL}-c_t) \end{bmatrix}, \tag{8}$$

$$\begin{bmatrix} T_{11} & T_{12} \\ T_{21} & T_{22} \end{bmatrix} = \frac{4}{\Delta} \left[(1+g) \begin{bmatrix} c_{iR}(c_{iL}+c_t) & 0 \\ 0 & c_{iL}(c_{iR}+c_t) \end{bmatrix} + (1-g) \begin{bmatrix} 0 & c_{iL}(c_{iR}-c_t) \\ c_{iR}(c_{iL}-c_t) & 0 \end{bmatrix} \right], \tag{9}$$

where R'_{ij} and T'_{ij} with $i = 1,2$ and $j = 1,2$ denote the co-polarized and cross-polarized reflection and transmission coefficients, respectively. And we have $c_{iR} = \cos\theta_{iR}$, $c_{iL} = \cos\theta_{iL}$, $c_t = \cos\theta_t$, $g = \sqrt{\varepsilon_a/\mu_a\varepsilon_c/\mu_c + \mu_a\gamma_c^2}$, $A = 2c_t(c_{iR}-c_{iL})(1-g)^2$, $B = 4c_t(1-g^2)$, and $\Delta = (1+g)^2(c_{iR}+c_t)(c_{iL}+c_t) - (1-g)^2(c_{iR}-c_t)(c_{iL}-c_t)$.

3. Power relation at the interface between IAM and ICM

For a time-harmonic electromagnetic field, the time-averaged active power flow per unit area is defined to be

$$\langle \boldsymbol{S} \rangle = \frac{1}{2}\mathrm{Re}(\boldsymbol{E} \times \boldsymbol{H}^*) = \frac{|\boldsymbol{E}_0|^2}{2Z_a(Z_c)}\boldsymbol{k}, \tag{10}$$

where Re indicates the real part of the vector product $\boldsymbol{E} \times \boldsymbol{H}^*$, $Z_a = \sqrt{\mu_a/\varepsilon_a}$ and $Z_c = 1/\sqrt{\varepsilon_c/\mu_c + \gamma_c^2}$ denote the intrinsic impedances of a dielectric medium and a chiral medium, respectively, $\boldsymbol{k}$ indicates a unit vector parallel to $\boldsymbol{E} \times \boldsymbol{H}^*$. The formula in Eq. (10) is commonly used for the calculation of electromagnetic energy.

According to the energy conservation law, the normal components of the time-averaged energy flow incident on an interface must be equal to those leaving the interface. There is

$$(\langle \boldsymbol{S}_i \rangle + \langle \boldsymbol{S}_r \rangle - \langle \boldsymbol{S}_{t,RCP} \rangle - \langle \boldsymbol{S}_{t.LCP} \rangle) \cdot \boldsymbol{n} = 0, \tag{11}$$

where $\langle \boldsymbol{S}_i \rangle$, $\langle \boldsymbol{S}_r \rangle$, $\langle \boldsymbol{S}_{t,RCP} \rangle$, and $\langle \boldsymbol{S}_{t,LCP} \rangle$ denote the time average power of the incident, the reflected, and the transmitted waves, respectively. $\boldsymbol{n}$ is a unit vector perpendicular to the interface.

The reflection power coefficient is defined as

$$\begin{aligned} r &= -\frac{\langle \boldsymbol{S}_r \rangle \cdot \boldsymbol{n}}{\langle \boldsymbol{S}_i \rangle \cdot \boldsymbol{n}} \\ &= \frac{|R_{12} + R_{11}\tan\alpha|^2 + |R_{22} + R_{21}\tan\alpha|^2}{1 + \tan^2\alpha}, \end{aligned} \tag{12}$$

where $\alpha = 0$ and $\alpha = \pi/2$ indicate the parallel and vertical polarized incident waves, respectively.

The transmission power coefficients are defined as

$$t_{RCP} = \frac{\langle \boldsymbol{S}_{t,RCP} \rangle \cdot \boldsymbol{n}}{\langle \boldsymbol{S}_i \rangle \cdot \boldsymbol{n}} = \frac{g\cos\theta_R\,|T_{12} + T_{11}\tan\alpha|^2}{\cos\theta_i\,(1+\tan^2\alpha)}, \tag{13}$$

$$t_{LCP} = \frac{\langle \boldsymbol{S}_{t,LCP} \rangle \cdot \boldsymbol{n}}{\langle \boldsymbol{S}_i \rangle \cdot \boldsymbol{n}} = \frac{g\cos\theta_L\,|T_{22} + T_{21}\tan\alpha|^2}{\cos\theta_i\,(1+\tan^2\alpha)}, \tag{14}$$

where t_{RCP} and t_{LCP} denote the transmission power coefficients of the RCP and LCP waves, respectively. $g = Z_a/Z_c$ is a shorthand notation.

It follows from Eq. (11) that

$$r + t_{RCP} + t_{LCP} = 1. \tag{15}$$

When an RCP (LCP) wave incidents upon an ICM–IAM interface, the normal component of the time-averaged energy

at the interface satisfies the law of conservation of energy; that is

$$\left(\left\langle \boldsymbol{S}_{\mathrm{i,RCP(LCP)}}\right\rangle + \langle \boldsymbol{S}_{\mathrm{r,RCP}}\rangle + \langle \boldsymbol{S}_{\mathrm{r,LCP}}\rangle - \langle \boldsymbol{S}_{\mathrm{t}}\rangle\right)\cdot \boldsymbol{n} = 0. \quad (16)$$

The reflection power coefficients are given as

$$r'_{\mathrm{RCP}} = -\frac{\left(\langle \boldsymbol{S}_{\mathrm{r,RCP}}\rangle + \langle \boldsymbol{S}_{\mathrm{r,LCP}}\rangle\right)\cdot \boldsymbol{n}}{\left\langle \boldsymbol{S}_{\mathrm{i,RCP}}\right\rangle \cdot \boldsymbol{n}} = \left|R'_{11}\right|^2 + \frac{\cos\theta_{\mathrm{L}}}{\cos\theta_{\mathrm{R}}}\left|R'_{21}\right|^2, \quad (17)$$

$$r'_{\mathrm{LCP}} = -\frac{\left(\langle \boldsymbol{S}_{\mathrm{r,RCP}}\rangle + \langle \boldsymbol{S}_{\mathrm{r,LCP}}\rangle\right)\cdot \boldsymbol{n}}{\left\langle \boldsymbol{S}_{\mathrm{i,LCP}}\right\rangle \cdot \boldsymbol{n}} = \frac{\cos\theta_{\mathrm{R}}}{\cos\theta_{\mathrm{L}}}\left|R'_{12}\right|^2 + \left|R'_{22}\right|^2, \quad (18)$$

where r'_{RCP} and r'_{LCP} denote the reflection power coefficients of the RCP and LCP waves, respectively.

The transmission power coefficients corresponding to the RCP and LCP waves can be written as

$$t'_{\mathrm{RCP}} = \frac{\langle \boldsymbol{S}_{\mathrm{t}}\rangle \cdot \boldsymbol{n}}{\left\langle \boldsymbol{S}_{\mathrm{i,RCP}}\right\rangle \cdot \boldsymbol{n}} = \frac{\cos\theta_{\mathrm{t}}\left(\left|T'_{11}\right|^2 + \left|T'_{21}\right|^2\right)}{g\cos\theta_{\mathrm{R}}}, \quad (19)$$

$$t'_{\mathrm{LCP}} = \frac{\langle \boldsymbol{S}_{\mathrm{t}}\rangle \cdot \boldsymbol{n}}{\left\langle \boldsymbol{S}_{\mathrm{i,LCP}}\right\rangle \cdot \boldsymbol{n}} = \frac{\cos\theta_{\mathrm{t}}\left(\left|T'_{12}\right|^2 + \left|T'_{22}\right|^2\right)}{g\cos\theta_{\mathrm{L}}}, \quad (20)$$

where t'_{RCP} and t'_{LCP} denote the transmission power coefficients of the RCP and LCP waves, respectively.

It can be derived from Eq. (16) that

$$r'_{\mathrm{RCP}} + t'_{\mathrm{RCP}} = 1. \quad (21)$$

$$r'_{\mathrm{LCP}} + t'_{\mathrm{LCP}} = 1. \quad (22)$$

4. Numerical results and discussions

To investigate the properties of reflection and transmission at a planar interface of IAM and ICM, three different cases: $k_{\mathrm{i(t)}} < k_{\mathrm{c}}$, $k_{\mathrm{i(t)}} > k_{\mathrm{c}}$, and impedance matching $Z_{\mathrm{a}} = Z_{\mathrm{c}}$, are taken into consideration in this section. The permeability of the ICM is selected to be identical to that of the IAM in the following discussions ($\mu_{\mathrm{a}} = \mu_{\mathrm{c}} = \mu_0$). A linearly polarized incident plane wave of arbitrary polarization is considered for the ICM–IAM interface, and an incident RCP plane wave is assumed for the ICM–IAM interface.

4.1. Reflection and transmission at an IAM–ICM interface

Case 1: $k_{\mathrm{i}} < k_{\mathrm{c}}$

In Fig. 2, the behavior of reflected wave at an IAM–ICM interface is studied, the parameters are $\varepsilon_{\mathrm{a}} = \varepsilon_0$, $\varepsilon_{\mathrm{c}} = 4\varepsilon_0$, and $\gamma_{\mathrm{c}} = 10^{-3}$. We have $\gamma_{\mathrm{c0}} = 3.98 \times 10^{-3}$ in this case, thus $\gamma_{\mathrm{c}} < \gamma_{\mathrm{c0}}$ ad $k_{\mathrm{i}} < k_{\mathrm{L}} < k_{\mathrm{R}}$ are obtained, which indicate that both the RCP and LCP waves propagate inside the chiral medium over the whole range of incidence angle. It can be seen from Fig. 2(a) that the cross-polarized reflection coefficients are significantly less than the co-polarized ones. When $\theta_{\mathrm{i}} = 64.33°$, the result shows that $|R_{22}| = 0$, which indicates that parallel polarization component of the reflected wave is generated by the vertically polarized incident wave. The normalized power of the reflected wave is presented in Fig. 2(b). It is clear that the value of the reflection power coefficient increases with the increase of the azimuthal angle from 0° to 90°. The results show that the contribution of the vertical polarized incident wave to the reflection power is larger than that of the parallel polarized incident wave.

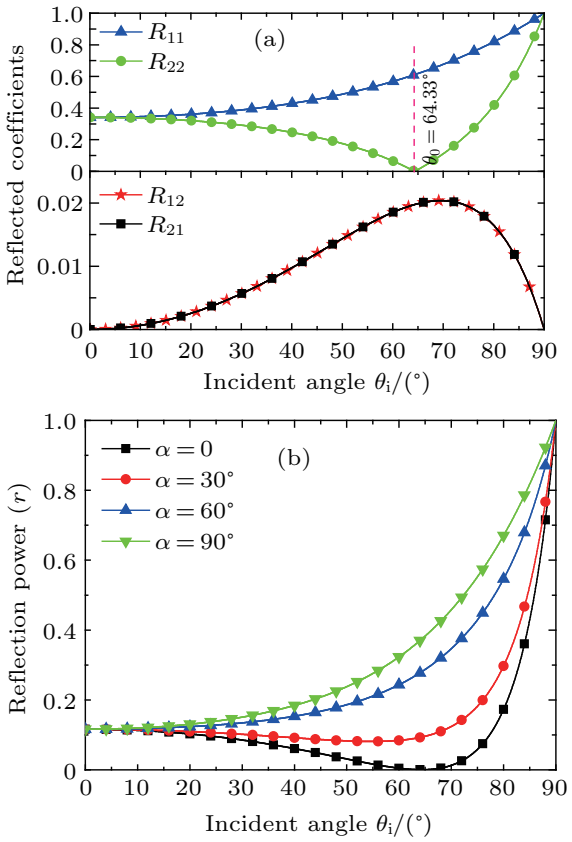


Fig. 2. Reflection coefficients and reflection power *versus* the incidence angle at an IAM–ICM interface: $\varepsilon_{\mathrm{a}} = \varepsilon_0$, $\varepsilon_{\mathrm{c}} = 4\varepsilon_0$, $\gamma_{\mathrm{c}} = 10^{-3}$.

The normalized powers of the reflected and transmitted waves as a function of the incidence angle are shown in Fig. 3, the parameters of the media are given by $\varepsilon_{\mathrm{a}} = \varepsilon_0$, $\varepsilon_{\mathrm{c}} = 4\varepsilon_0$, $\gamma_{\mathrm{c}} = 10^{-2}$. Thus, $\gamma_{\mathrm{c}} > \gamma_{\mathrm{c0}}$ and $k_{\mathrm{L}} < k_{\mathrm{i}} < k_{\mathrm{R}}$ are obtained. It can be observed from the diagrams that all the power coefficients grow or diminish at first and then reach to an extremum at $\theta_{\mathrm{i}} = \theta_{\mathrm{cL}}$, and power variation of the reflected wave is completely opposite to that of the RCP transmitted wave. This result shows that the azimuthal angle has strong effects on the power coefficients of the reflected and the RCP waves, but has a slight effect on that of the LCP wave. When the incidence angle θ_{i} exceeds the critical angle θ_{cL}, the LCP wave travels as a surface wave, thus power coefficient of the LCP wave goes to zero, whereas no dependence of LCP power on the azimuthal angle is observed.

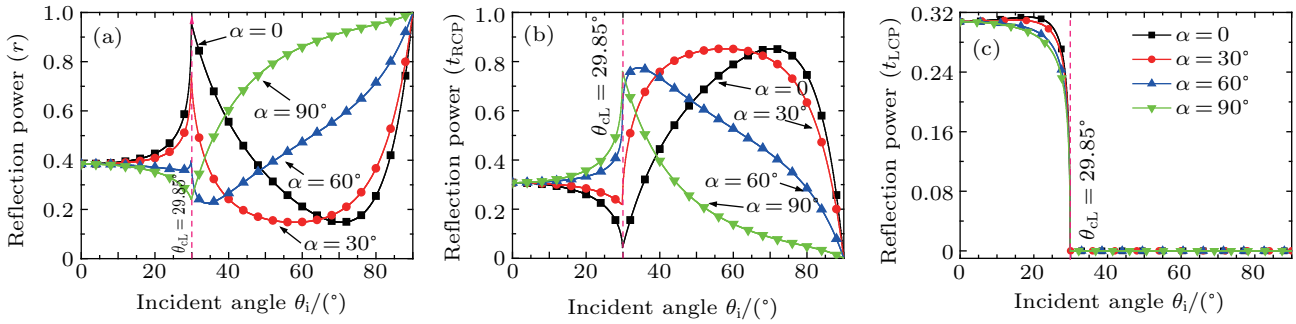


Fig. 3. Power reflection and transmission coefficients *versus* the incidence angle at an IAM–ICM interface, $\varepsilon_a = \varepsilon_0$, $\varepsilon_c = 4\varepsilon_0$, $\gamma_c = 10^{-2}$. (a) Reflection power, (b) transmission power of RCP wave, (c) transmission power of LCP wave.

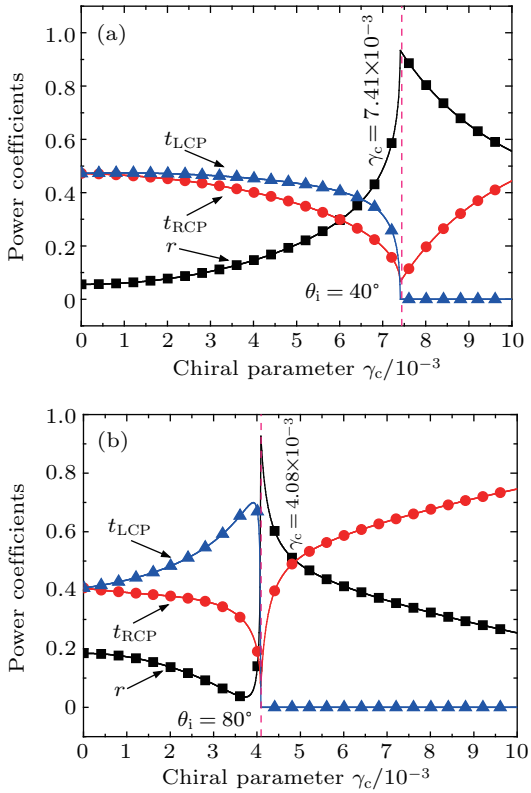


Fig. 4. Power reflection and transmission coefficients *versus* the chiral parameters with $\varepsilon_a = \varepsilon_0$, $\varepsilon_c = 4\varepsilon_0$ at $\theta_i = 40°$, and $\theta_i = 80°$, respectively.

Effects of the chiral parameters on power normalized coefficients at two different incident angles are investigated in Fig. 4. There is $k_i < k_L < k_R$ for γ_c varying from 0 to γ_{c0}, both the RCP and LCP waves propagate normally in this case. Whereas if $\gamma_c > \gamma_{c0}$, we have $k_L < k_i < k_R$, and the LCP power coefficients go to zero at $\theta_i = \theta_{cL}$. Therefore, when the value of chiral parameters are 7.41×10^{-3} and 4.08×10^{-3} in Figs. 4(a) and 4(b), respectively, the corresponding incidence angles, $\theta_i = 40°$ and $80°$, are the so-called critical angles. From these data, it can be concluded that the chiral parameter diminishes with the increase of the critical angle in this case. When the incidence angle $\theta_i \to 90°$, the chiral parameter approaches to $\gamma_{c0} = 3.98 \times 10^{-3}$.

Case 2: $Z_a = Z_c$

As shown in Fig. 5, the properties of both the reflected and the transmitted waves against the incidence angle are investigated. The parameters of the two media are $\varepsilon_a = 4\varepsilon_0$, $\varepsilon_c = \varepsilon_a - \mu_c \cdot \gamma_c^2$, and $\gamma_c = 10^{-3}$. In this case, $k_R > k_i > k_L$ and $Z_a = Z_c$ are available, thus an impedance matching condition between the chiral and achiral media is achieved. It is clear from Figs. 5(a) and 5(b) that $|R_{11}| = |R_{22}|$, $|R_{12}| = |R_{21}|$, $|T_{11}| = |T_{12}|$, $|T_{21}| = |T_{22}|$ are obtained. Variations of power coefficients with the incidence angle are also investigated in Fig. 5(c). When $\theta_i < \theta_{cL}$, the value of the reflection power coefficient is very small, therefore most of the incident power is transmitted to the achiral medium. As the incident angle approaches the critical angle of incidence, the reflection power grows rapidly and increases up to 0.5 at $\theta_i = \theta_{cL}$, while the transmission power of LCP wave diminishes rapidly and goes to zero at the critical angle. For $\theta_i > \theta_{cL}$, the reflection power is still on the increase whereas the LCP wave is changed into a surface polarized mode. Furthermore, both the power reflection and transmission coefficients are also calculated for a monochromatic incident plane wave with $\alpha = 45°$, $60°$. The numerical data lead us to conclude that power coefficients of the reflected and transmitted waves are independent of the polarization state of the incidence wave in the case of impedance matching condition.

Case 3: $k_i > k_c$

Figure 6 shows the behavior of both the reflection and transmission powers against the incidence angle. The parameters are $\varepsilon_a = 4\varepsilon_0$, $\varepsilon_c = \varepsilon_0$, $\gamma_c = 10^{-3}$. We have $k_i > k_R > k_L$ in this case. From Eq. (7), we have $\theta_{cL} = 20.24°$ and $\theta_{cR} = 46.28°$ for the LCP and the RCP waves, respectively. It can be seen that both the power reflection and transmission coefficients have an extremum at the critical angle. The powers of the reflected and transmitted waves are calculated at $\alpha_i = 0°$, $30°$, $60°$, and $90°$, respectively. It can be seen from Fig. 6 that there is a significant difference of the reflection and RCP power curves for different azimuthal angles, while no dependence of LCP power on the polarization of the incidence wave is observed. If $\theta_i > \theta_{cR}$, the reflection power coefficient close to unit, and the transmission power goes to zero, then the phenomenon of total internal reflection takes place.

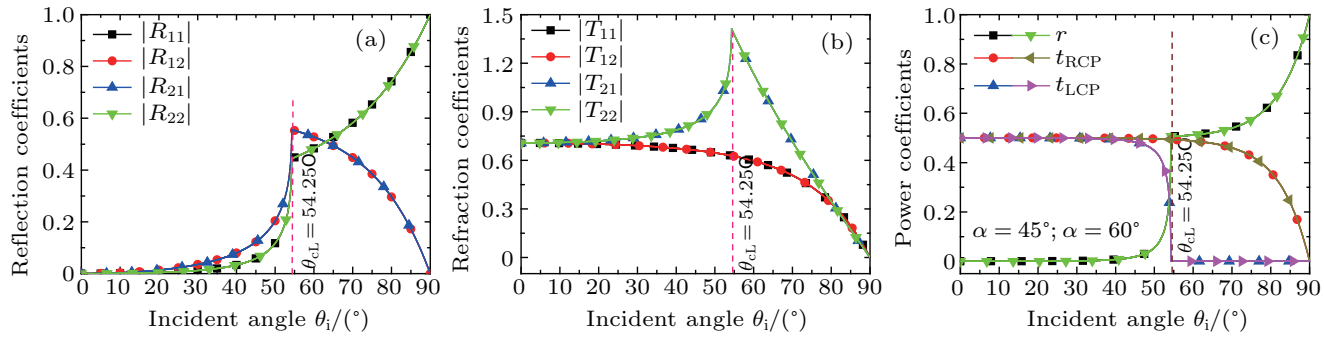


Fig. 5. Reflection and transmission properties at an IAM–ICM interface under impedance matching condition, $\varepsilon_{\mathrm{a}} = 4\varepsilon_0$, $\gamma_{\mathrm{c}} = 10^{-3}$, $\varepsilon_{\mathrm{c}} = \varepsilon_{\mathrm{a}} - \mu_{\mathrm{c}} \cdot \gamma_{\mathrm{c}}^2$.

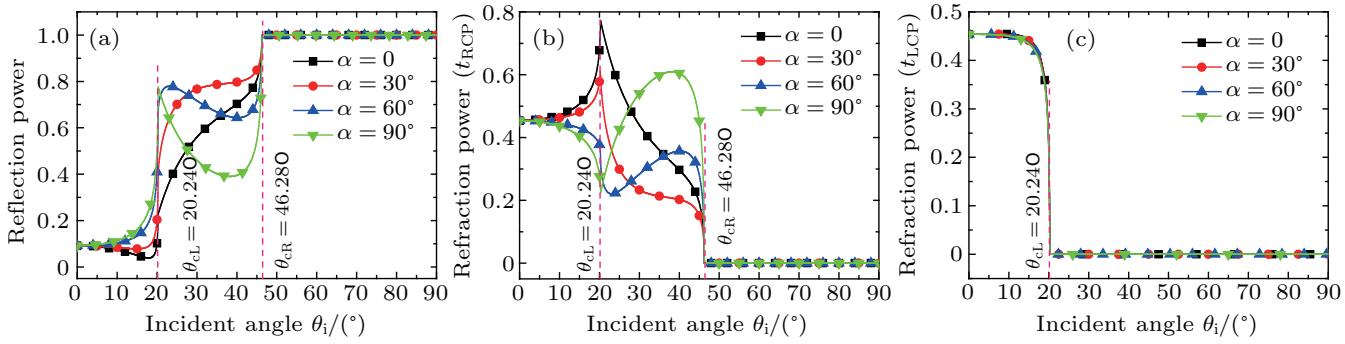


Fig. 6. Reflection and transmission powers *versus* the incidence angle at an IAM–ICM interface, $\varepsilon_{\mathrm{a}} = 4\varepsilon_0$, $\varepsilon_{\mathrm{c}} = \varepsilon_0$, $\gamma_{\mathrm{c}} = 10^{-3}$.

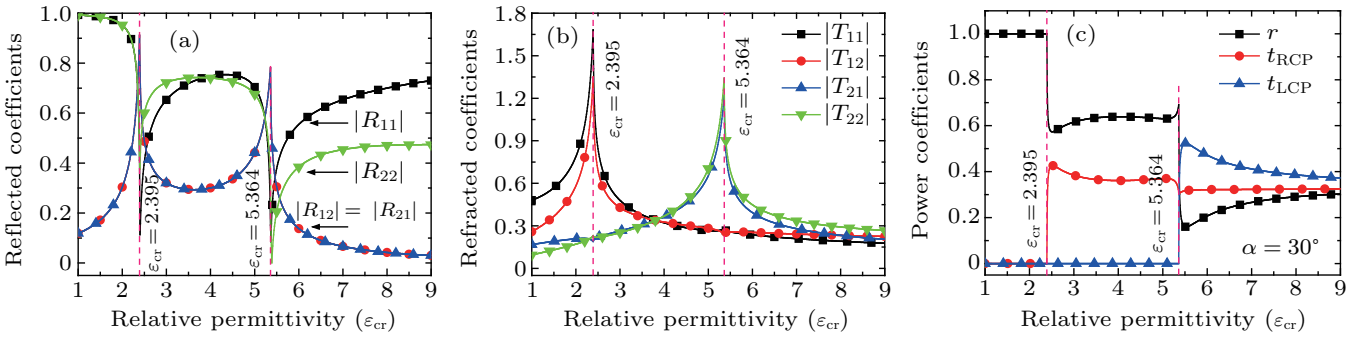


Fig. 7. Characteristics of the reflected and transmitted waves *versus* the relative permittivity $\varepsilon_{\mathrm{cr}}$ at an IAM–ICM interface: $\varepsilon_{\mathrm{a}} = 4\varepsilon_0$, $\gamma_{\mathrm{c}} = 10^{-3}$.

Figure 7 shows the characteristics of the reflected and transmitted waves *versus* the relative permittivities $\varepsilon_{\mathrm{cr}}$ of the chiral medium at $\theta_{\mathrm{i}} = 80°$. The parameters are given by $\varepsilon_{\mathrm{a}} = 4\varepsilon_0$, $\gamma_{\mathrm{c}} = 10^{-3}$. The result shows that there is one, or two, or none of the transmitted waves propagating inside the chiral medium as $\varepsilon_{\mathrm{cr}}$ varies from 1 to 9, and variation of the co-polarized reflection coefficient is completely opposite to that of the cross-polarized one. For $\varepsilon_{\mathrm{cr}} < 2.395$, both the critical angles θ_{cR} and θ_{cL} are less than the assumed incidence angle, neither of the transmitted wave propagates, the transmission power approaches to zero. If $2.395 < \varepsilon_{\mathrm{cr}} < 5.364$, then there is $k_{\mathrm{L}} < k_{\mathrm{i}} < k_{\mathrm{R}}$ and $\theta_{\mathrm{i}} > \theta_{\mathrm{cL}}$, only the transmitted RCP wave exists inside the chiral medium, whereas if $\varepsilon_{\mathrm{cr}} > 5.364$, we have $k_{\mathrm{i}} < k_{\mathrm{L}} < k_{\mathrm{R}}$, then both the two transmitted waves propagate normally.

4.2. Reflection and transmission at an ICM–IAM interface

Power reflection and transmission coefficients against the incidence angle for the case of $k_{\mathrm{t}} < k_{\mathrm{c}}$ and $k_{\mathrm{t}} > k_{\mathrm{c}}$ are shown in Figs. 8(a) and 8(b), respectively. In Fig. 8(a), there is $k_{\mathrm{t}} < k_{\mathrm{L}} < k_{\mathrm{R}}$, For $\theta_{\mathrm{i}} < \theta_{\mathrm{cR}}$, though both the reflected and transmitted waves can propagate normally, the reflected power r'_{RCP} is much less than the transmitted power t'_{RCP}. Whereas if $\theta_{\mathrm{i}} > \theta_{\mathrm{cR}}$, the transmitted wave becomes evanescent, the normalized transmitted power goes to zero. In Fig. 8(b), we have $\gamma_{\mathrm{c}} < \gamma_{\mathrm{c0}}$ and $k_{\mathrm{L}} < k_{\mathrm{R}} < k_{\mathrm{t}}$, the results show that the value of the reflected power is very small for $\theta_{\mathrm{i}} < \theta_{\mathrm{c}}$, which indicates that most of the incident power is transmitted to the achiral medium. When $\theta_{\mathrm{i}} > \theta_{\mathrm{c}}$, the LCP reflected wave becomes evanescent, the reflection power approaches to zero at first and then increases with the increase of incidence angle, and ultimately reaches unity as $\theta_{\mathrm{i}} \to 90°$.

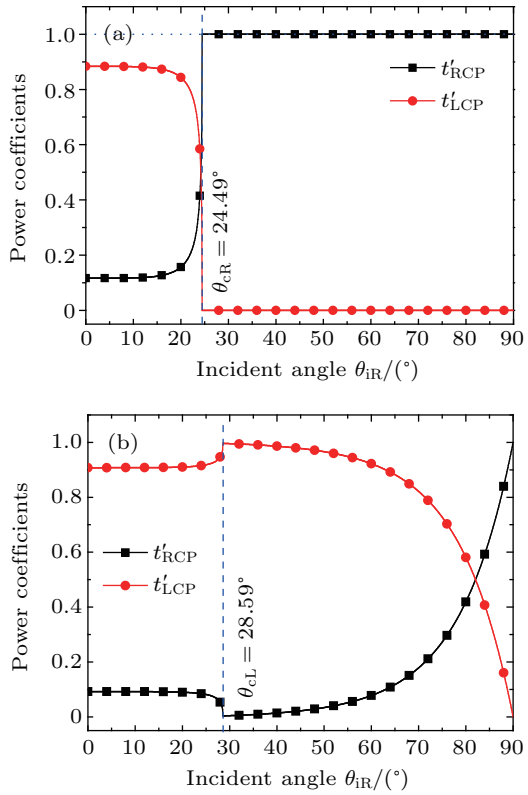


Fig. 8. Characteristics of the reflected and transmitted waves *versus* the incidence angle at an ICM–IAM interface for an RCP incident wave: (a) $\varepsilon_{\rm a} = \varepsilon_0$, $\varepsilon_{\rm c} = 4\varepsilon_0$, $\gamma_{\rm c} = 10^{-3}$; (b) $\varepsilon_{\rm a} = 4\varepsilon_0$, $\varepsilon_{\rm c} = \varepsilon_0$, $\gamma_{\rm c} = 10^{-3}$.

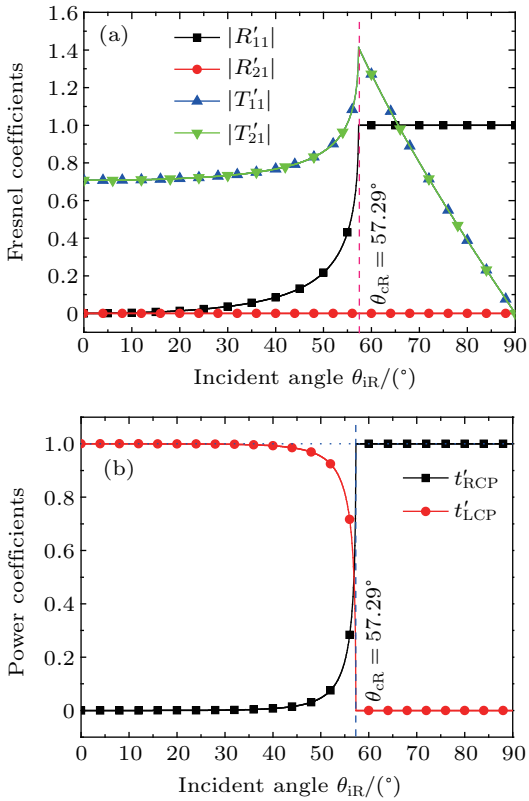


Fig. 9. Characteristics of the reflected and transmitted waves *versus* the incidence angle at an ICM–IAM interface for an RCP incident wave: $\varepsilon_{\rm a} = 4\varepsilon_0$, $\varepsilon_{\rm c} = \varepsilon_{\rm a} - \mu_{\rm c}\gamma_{\rm c}^2$, $\gamma_{\rm c} = 10^{-3}$.

In Fig. 9, the impedance matching between the chiral and the achiral medium can be achieved with the given parameters, which can be characterized by power coefficients of the reflected and transmitted waves. It is clear from Fig. 9(a) that $|R'_{11}|$ varies slowly at first with $\theta_{\rm iR}$ and then increases up to a maximum of 1 at $\theta_{\rm iR} = \theta_{\rm cR}$. For $\theta_{\rm iR} > \theta_{\rm cR}$, the coefficient $|R'_{11}|$ is always equal to unit. Both $|R'_{21}| = 0$ and $|T'_{11}| = |T'_{21}|$ are valid for the incidence angle from 0° to 90°. These data lead us to conclude that both the reflected and transmitted waves are of the same circular polarization state as the incident RCP plane wave in this case. Figure 9(b) shows that the reflection power coefficient is so small that it can be negligible to the case of a wide range of incidence angle $\theta_{\rm iR} < \theta_{\rm cR}$, which shows that the chiral medium exhibits high transmission and impedance matching to the achiral medium. whereas if the angle of incidence exceeds the critical angle, there is $t'_{\rm RCP} = 0$, the phenomenon of total internal reflection occurs.

5. Conclusion and perspectives

This paper begins with a discussion of wave propagation inside the chiral medium, followed by an analysis of the relations among the normal components of the time-averaged Poynting vectors of the incident, the reflected, and the transmitted waves. Theoretical formulas of the normalized reflection power and the transmission power at an IAM–ICM interface are obtained for an incident plane wave with arbitrary polarization, as well as those at an ICM–IAM interface for an RCP/LCP incident wave. The magnitudes of the Fresnel coefficients, the reflection power, and the transmission power for three different cases are calculated, and effects of the incidence angle, the chiral parameter, and the permittivity on the characteristics of the power reflection and transmission coefficients are investigated.

Our numerical results show that behaviours of the transmitted waves vary significantly with the change of the incidence angle, the permittivity, and the chiral parameter. Furthermore, the azimuthal angle has strong effects on the transmitted power of the RCP wave and reflection power, while it has a slight influence on the transmitted power of the LCP wave. It is noted that high transmission is always exhibited as the incidence angle less than the critical angle under the impedance matching condition. In the case of an IAM–ICM interface, power reflection and transmission coefficients are independent of the polarization state of the incidence wave. As for the case of an ICM–IAM interface, both the reflected and transmitted plane waves have the same circular polarization state as the incident wave.

References

[1] Jaggard D L, Mickelson A R and Papas C H 1979 *Appl. Phys.* **18** 211
[2] Engheta N and Jaggard D L 1988 *IEEE Anten. Propag. Soc. Newslett.* **30** 6
[3] Cory H 2012 *J. Electromagn. Waves Appl.* **9** 805
[4] Liao S B and Yin G J 1993 *Appl. Phys. Lett.* **62** 2480

[5] Jin Y and He S L 2005 *Opt. Express* **13** 4974
[6] Plum E and Zheludev N I 2015 *Appl. Phys. Lett.* **106** 221901
[7] Bohren C F 1974 *Chem. Phys. Lett.* **29** 458
[8] Cupis P D 2006 *Opt. Commun.* **261** 203
[9] Athanasiadis C 2005 *Math. Anal. Appl.* **309** 517
[10] Zhu X P, Liao T Q and Zhang H Y 2012 *J. Quantum Spectrosc. Radiat.* **113** 1946
[11] Pendry J B 2004 *Science* **306** 1353
[12] Wongkasem N, Akyurtlu A, Marx K A, Dong Q, Li J and Goodhue W D 2007 *IEEE Trans. Anten. Propag.* **55** 3052
[13] Bassiri S, Papas C H and Engheta N 1988 *J. Opt. Soc. Am. A* **5** 1450
[14] Cory H and Rosenhouse I 1991 *J. Mod. Opt.* **38** 1229
[15] Cory H and Rosenhouse I 1992 *J. Mod. Opt.* **39** 1321
[16] Crittenden P E and Bahar E 2005 *Can. J. Phys.* **83** 1267
[17] Ali W, Ahmad F, Syed A A and Naqvi Q A 2015 *J. Electromagn. Waves Appl.* **29** 525
[18] Cumali S and Savas U 2006 *Sci. China Ser. E* **49** 457
[19] Liu B and Dong J F 2007 *Optoelectron. Lett.* **3** 0462
[20] Dong J F and Li J 2013 *Optoelectron. Lett.* **9** 0148
[21] Ghaffar A and Alkanhal M A S 2015 *Wave Random Complex* **25** 18
[22] Dong J F and Li J 2012 *Prog. Electromagn. Res.* **127** 389
[23] Chen H Y, Li J Z, Lu X W and Xu S X 2012 *Opt. Commun.* **285** 1
[24] Lekner J 1996 *Pure Appl. Opt.* **5** 417
[25] Georgieva E 1995 *J. Opt. Soc. Am. A* **12** 2203
[26] Xu G D, Zang T C, Mao H M and Pan T 2011 *Phys. Rev. A* **83** 053828
[27] Yan B, Zhang H Y and Zhang J Y 2016 *Appl. Phys. B* **122** 1
[28] Lakhtakia A, Varadan V V and Varadan V K 1990 *J. Opt. Soc. Am. A* **7** 1654
[29] Tang Q, Meng F Y, Zhang K, Wu K and Li L W 2011 *Acta Phys. Sin.* **60** 014206 (in Chinese)
[30] Li Z J, Xiong Y S, Liu Z L and Yao K L 1998 *Chin. Phys. B* **7** 432
[31] Li Z J, Xiong Y S, Liu Z L and Yao K L 1997 *Chin. Phys. B* **6** 731
[32] Zheng Y D, Li J Q and Li C F 2002 *Chin. Phys. Lett.* **19** 791
[33] Li Y F, Zhang J Q, Qu S B, Wang J F, Zheng L, Zhou H, Xu Z and Zhang A X 2015 *Chin. Phys. B* **24** 014202
[34] Condon E U 1937 *Rev. Mod. Phys.* **9** 432
[35] Lakhtakia A, Varadan V K and Varadan V V 1989 *Lect. Notes Phys.* **335** 395
[36] Sihvola A H and Lindell I V 1991 *Microwave Opt. Technol. Lett.* **4** 295